

**Energy Focus**

**Noninvasive acoustic sensing diagnoses lithium-ion battery health**

Lithium-ion batteries near-universally serve as power sources in portable electronics, and an increasing number of electric automobiles and trucks are appearing on roadways. All of these applications have a common element: the batteries that power them wear down with time and use. As lithium-ion cells repeatedly cycle, they generate several side reactions that preclude the electrodes from maintaining maximum storage capacity. Among the most damaging degradation processes is the proclivity for lithium ions, found in the cathode and electrolyte of the cell, to deposit on the surfaces of the graphite anodes in the form of bulk metal. This plating reaction blocks electrolyte ion mobilities and inhibits intercalation of lithium ions into the electrode during charging. Extreme temperatures and excessive rapid cycling rates exacerbate this energy-density fade. Moreover, needle-like growth of lithium-metal plates in the morphology of dendrites poses additional risks of short-circuiting cells. It is critical to have characterization techniques that can accurately detect and quantify this

phenomenon in a timely manner. Most previous approaches typically relied on postmortem analyses of disassembled cells. What is needed is real-time (*in operando*) assessment of battery health.

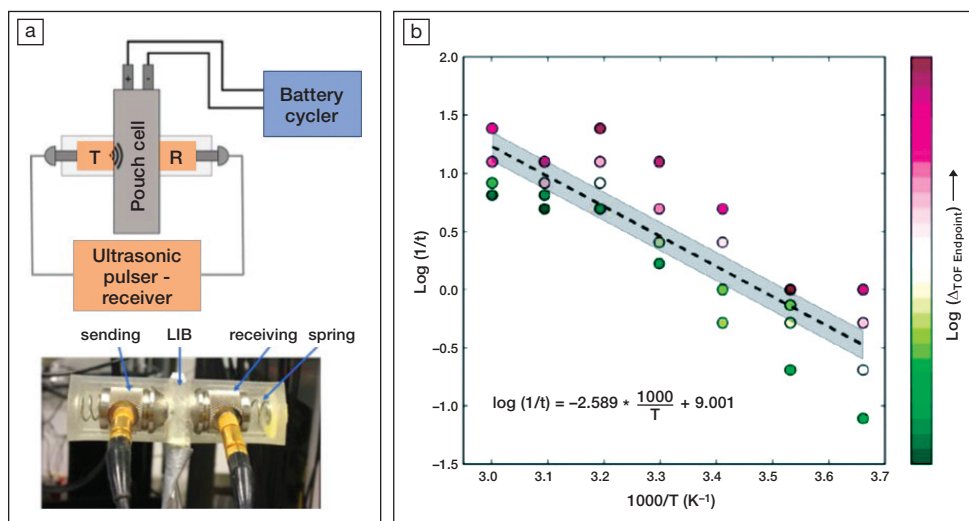
In order to develop a nondestructive and more precise diagnostic method, Daniel Steingart of Columbia University and his colleagues at Columbia and Princeton Universities took advantage of the fact that density variations in solids alter the speed of sound as it travels through them. The researchers pinged cycled commercial lithium-ion pouch cells with ultrasonic signals and analyzed the wave forms of the received signals. Intercalation of lithium into the graphite or plating on its surface changes the densities and modulus of the cell and thus alters the length of time it takes for the incident sound wave to return back to the analyzer. This is known as “time of flight.” The researchers identified the cycling and temperature conditions that induced lithium plating and corresponding time-of-flight measurements. They published their findings in a recent issue of *Cell Reports Physical Science* (doi:10.1016/j.xcrp.2020.100035).

Steingart says, “We think acoustics provide an important complement to existing characterization and diagnostic tools for batteries. The methods

and analyses we show in the paper are analogous to electrochemical impedance spectroscopy (EIS). Where EIS can be directly correlated to dynamics and provide inferences to structure, acoustic data are directly related to structure and provides inferences into dynamics.”

The researchers connected acoustic transducers across rectangular pouch cells and measured the changes in the wave period to derive times of flight. Their measurements specifically identified differences in acoustic shifts between those measured for slow charge cycles (that did not deposit lithium metal on electrodes) and faster, plating-inducing charging. The efforts carefully deconvoluted time-of-flight-induced changes due to plating from other battery degradation processing, such as gas evolution and swelling of pouch cells. Research team members coupled the acoustic measurements with electrochemical measurements and used postmortem analysis of cycled cells with microscopy and crystallographic analysis to confirm the plating behavior. Of note, the researchers derived an Arrhenius (logarithmic–logarithmic) relationship between the rate of bulk lithium plating, cell charging current, and the temperature of the battery.

US Naval Research Laboratory researchers, who are unaffiliated with this effort, assessed its significance. Corey Love says, “Improving lithium battery safety requires multiple diagnostic inputs to provide a comprehensive understanding of battery state of health and stability. Ultimately, a collection of electrochemical diagnostics coupled with innovative methods like Steingart’s are needed to identify potentially harmful events, like lithium plating, but also the interplay between electrochemical processes and mechanical and thermal effects.” Rachel Carter adds, “From a diagnostics perspective, it is exciting that the acoustic strategy is sensitive to lithium deposit morphology and quantity,



(a) The researchers developed an acoustic sensing setup that determined changes in time-of-flight to derive degree of lithium plating on graphite anodes after cycling. LIB is Li-ion battery. (b) These measurements delivered an Arrhenius relationship between cycling temperature, charge rate, and plating-induced electrode health decay. Logarithmic color bar represents measured time-of-flight differences detected by acoustic sensing. Credit: Daniel Steingart.



enabling risk assessment, which is difficult to achieve with the EIS analysis.”

Unlike other characterization tools, acoustic sensing is noninvasive, diagnoses specific segments of battery cells, and aptly discerns between different degradation mechanisms. This approach will

provide valuable fundamental insight into optimal temperature and charge/discharge regimes for novel battery designs, according to the research team. Most importantly, the required diagnostic equipment is relatively compact and simple. This allows many cells to be tested in the laboratory at

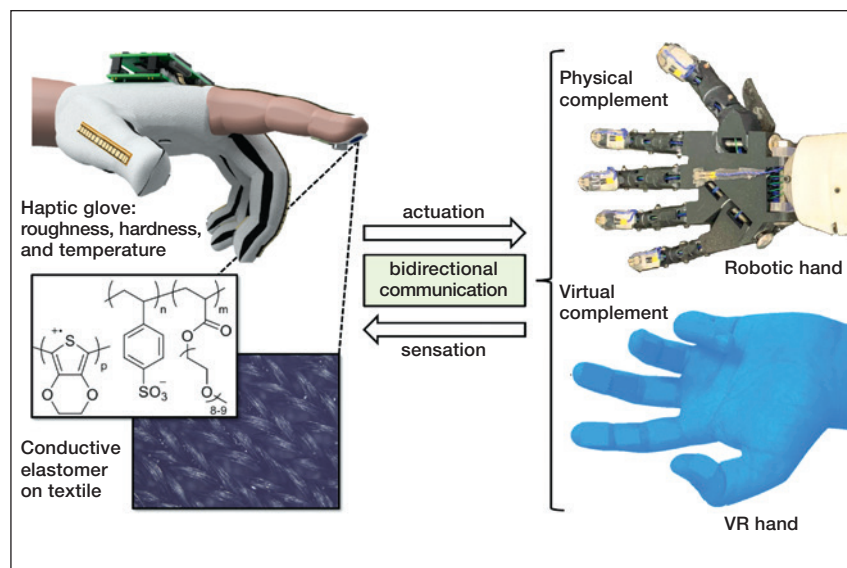
once, and eventually electric transportation vehicles and grid-scale battery banks will stand to benefit from built-in sensors that will provide real-time tracking of battery health and warn about impending degradation or safety concerns.

**Boris Dyatkin**

### Controlled radical polymerization enables sense of texture in haptics

Kinesthetic communication represents a key area of interest in perfecting user experience in virtual reality (VR) applications through creating texture sensation on fingertips. Haptic technology has been used to deliver the feeling of surface roughness, hardness, and temperature by a mixed mode of mechanical and electrical stimulation. However, nonfunctional homogeneous materials and bulky actuators pose spatial limitations on the controllability of the sensation gamut, thus deviating from the experience of real touch. Stimuli-responsive polymers synthesized by controlled free-radical polymerization over narrow molecular weight and polydispersity suggest a potential route for modifying tactile sensation at the molecular level by proper materials design and selection.

In a recent issue of *Advanced Intelligent Systems* (doi:10.1002/aisy.202000018), a research team, led by Darren Lipomi at the University of California, San Diego, reported the use of aqueous reversible addition fragmentation transfer polymerization based on  $\pi$ -conjugated PEDOT, stretchable scaffold PSS, and an acrylic polymer, poly(ethylene glycol) methyl ether acrylate, to fabricate an elastomeric conductive block copolymer for electrohaptic stimulation. “This paper represents the first time the tools of materials chemistry have been applied to a problem in haptics,” says Lipomi. “We synthesized a stretchable, printable conductive polymer using controlled radical polymerization while most haptic actuators are made using commercial, off-the-shelf components.” The research team



Schematic drawings of the wireless multimodal haptic glove with electrohaptic sensor enabled by a synthesized conductive polymer for interfacing with a robotic hand and virtual reality (VR). Credit: *Advanced Intelligent Systems*.

developed a wireless multimodal haptic glove to recreate texture sensation when interfacing with a robotic hand or VR environment. The glove uses three types of actuators that produce electrohaptic for roughness, vibrotactile for hardness, and thermoelectric effect for temperature. The synthesized conductive polymer was used for electrohaptic stimulation due to its relatively high conductivity and low electrical impedance to metal electrodes.

The researchers also demonstrated the accuracy of tactile effect in psychophysical discrimination tasks in VR. Participants were asked to wear the haptic glove and evaluate the texture of test panels that appeared in the VR environment. Trained participants can achieve 98% accuracy in associating sensations while untrained participants have an accuracy of 85%. “What excites us in particular is the potential use of haptics

in medicine: medical training, robot-assisted procedures, physical therapy, and other forms of remote care for ‘health-care deserts,’” Lipomi says. “While we are quite far away from achieving these goals, we believe this invention is a useful contribution.”

“Solving the problem of displaying realistic sensations to users is the holy grail of haptics,” says Aadeel Akhtar, CEO and Founder of PSYONIC, Inc., a company developing sensorized prosthetic hands to enable amputees to feel. “The approach of using tools from organic chemistry is ingenious in developing realistic haptic interfaces that can interact at a molecular level with the skin. These methods expand the toolbox available to haptics researchers to further fine-tune the percepts users feel for more realistic sensations.”

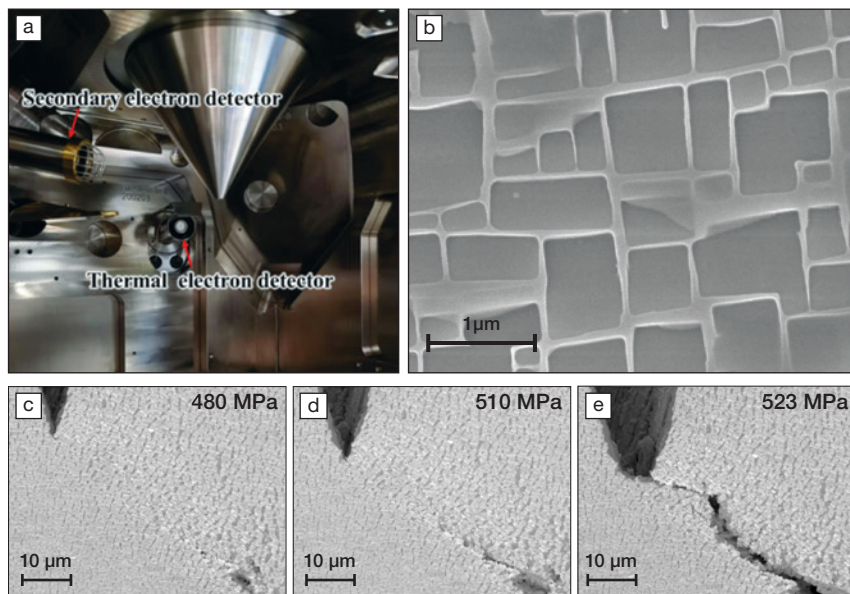
**YuHao Liu**

**In situ mechanical testing in an SEM performed at 1150°C with submicron resolution**

Metals and ceramics are widely used in high-temperature and other extreme environments; for example, boron carbides are used in nuclear reactors and nickel superalloys in turbine blades. For these applications, the materials need not only to withstand high temperatures but also to perform while retaining their mechanical properties. Although mechanical testing can be done at high temperatures, so far this has only been achieved on macroscopic specimens where the failure mechanisms are investigated post-mortem. To get nanoscopic and microscopic details, compression, tensile, or crack propagation tests can also be conducted inside a scanning electron microscope (SEM). However, simultaneously heating, deforming, and observing a sample within an SEM is challenging, where the thermal electrons emitted by a hot sample and the heating wire interact with the imaging electron beam and blur the images.

To retain the high resolutions in an SEM during heating, the research teams of Yuefei Zhang and Ze Zhang from Beijing University of Technology and Zhejiang University, China, developed a special *in situ* tensile setup that heats up to 1150°C while retaining force and displacement resolutions of 1 N and 0.08 μm, respectively. This development is detailed in an article published earlier this year in the *Review of Scientific Instruments* (doi:10.1063/1.5142807).

What makes the setup special is a multilayer tantalum metal shield that blocks the thermal radiation from the heated stage, as well as a procedure to suppress the interference between the thermal and the imaging electrons. Typically, a bias control is applied to the thermal shield plate using feedback from a thermal electron detector placed close to the secondary



(a) View of the interior of the scanning electron microscope (SEM) indicating the secondary thermal electron detectors. Credit: Yuefei Zhang. (b) Sub-micrometric resolution micrograph of the surface of a nickel superalloy at 1150°C (credit: AIP Publishing). (c–e) Snapshots of a notched superalloy sample deformed at 1150°C showing the crack propagation features under increasing stress. Credit: AIP Publishing.

electron detector of the SEM (Figure a). The local heating of the sample is done using a tungsten filament, whereas the setup is cooled using water.

After calibration procedures to correct for thermal expansion of the device itself, control tests were done using standard specimens made of carbon steel. The yield strength measured, 1129 MPa, showed an error of less than 2% compared to the reference value.

Finally, the setup was used to stretch at 1150°C a single-crystal Ni superalloy specimen with a notch on its side. The crack propagation and surface features were clearly revealed during the experiment (Figure b–e). The device was used to study the oxidation of nickel superalloys under thermo-stressed conditions in an SEM, and the results were published earlier this year in *Scientific Reports* (doi:10.1038/s41598-020-59968-3).

But the testing is not limited to metallic alloys. “Of course, it can be

used for nonmetallic samples too,” says Zhang. “When we observe ceramic samples at high-temperature conditions, the yield of secondary electron emission increases. This improves the image quality without the need for a conductive coating.”

The capabilities offered are exciting for many. “The developed instrument paves the way for exploring new mechanisms, which could serve as guidelines for designing ultra-tough ceramic nanocomposites for demanding environments,” says Christos Athanasiou from Brown University, who is investigating such materials but was not part of the study. “For example, silicon carbide ceramics reinforced with 2D-hexagonal boron nitride fail at the interface between matrix and reinforcement. This occurs during loading and crack bridging, but no one has looked at the failure mechanism at high temperatures.”

**Hortense Le Ferrand**

**Liven up your next virtual meeting!**



## Energy Focus

**Empirical equations identify metal–organic frameworks with unprecedented hydrogen-storage capacity**

Banglin Chen of The University of Texas at San Antonio and co-workers have developed empirical equations to predict the H<sub>2</sub>-storage capacity of metal–organic frameworks (MOFs), as they reported in a recent issue of *Advanced Materials* (doi:10.1002/adma.201907995). Their equations illustrate that suitable surface areas and/or pore volumes did lead to high H<sub>2</sub>-storage capacities.

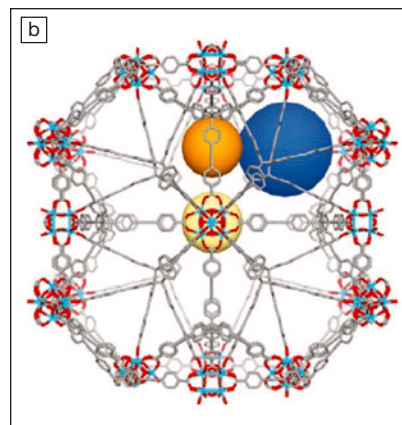
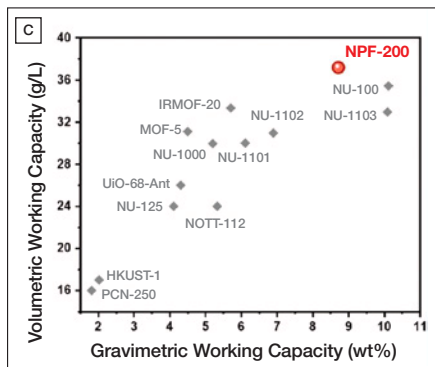
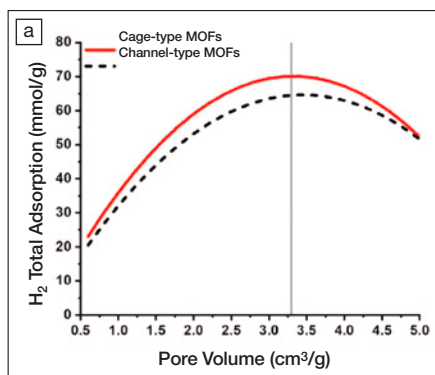
To derive the empirical equations, the researchers first calculated the pore volumes of six model MOFs for H<sub>2</sub> storage based on their crystal structures. Fitting the pore volumes with their experimental H<sub>2</sub>-storage capacities revealed a non-linear relationship between the two parameters. Specifically, under 100 bar and at 77 K, the total moles ( $n_{\text{total}}$ ) of H<sub>2</sub> stored in cage-type MOFs (MOFs having spherical pores) follow the equation:

$$n_{\text{total}} = 0.085V_p - 0.013V_p^2$$

and those of channel-type MOFs (MOFs having cylindrical pores) fit the equation:

$$n_{\text{total}} = 0.076V_p - 0.011V_p^2,$$

where  $V_p$  is pore volume. Both equations indicate that there was an optimal pore volume corresponding to maximal storage capacity. This relationship between  $n_{\text{total}}$  and  $V_p$  was associated with the pore size: Small pores bestow low H<sub>2</sub>-storage capacity as they offer limited storage space for H<sub>2</sub>. Large pores decrease the interaction potential between H<sub>2</sub> and MOFs, leading to reduced pore filling by H<sub>2</sub>. Cage-type MOFs stored more H<sub>2</sub> than channel-type MOFs at similar pore volumes because the former can interact with H<sub>2</sub> via more surface atoms than the latter, which allowed more H<sub>2</sub> adsorbed inside



(a) The predicted total moles of H<sub>2</sub> stored versus the pore volumes of metal–organic frameworks (MOFs). (b) Structure of NPF-200. The orange, light yellow, and blue spheres highlight three types of spherical pores in NPF-200. (c) Volumetric working capacity and gravimetric working capacity of NPF-200 at 77 K compared with other MOFs. Credit: *Advanced Materials*.

pores. The empirical equations predicted that cage-type MOFs with pore volumes around 2.0–4.0 cm<sup>3</sup> g<sup>−1</sup> would achieve the highest H<sub>2</sub>-storage capacity.

Guided by the equations, the researchers identified a promising MOF candidate for H<sub>2</sub>-storage, designated NPF-200. This Zr-containing, cage-type MOF had a pore volume of 2.17 cm<sup>3</sup> g<sup>−1</sup> and a high volumetric surface area of 2268 m<sup>2</sup> cm<sup>−3</sup>. High-pressure H<sub>2</sub> sorption demonstrated that 65.7 mmol H<sub>2</sub> was stored 1 g of NPF-200 at 77 K and 100 bar. This value only deviated 5.9% from the predicted value (61.8 mmol H<sub>2</sub> per gram of NPF-200). More outstandingly, the mass of H<sub>2</sub> released from NPF-200 when pressure was decreased from 100 bar to 5 bar at 77 K reached 37.2 g L<sup>−1</sup>, which was better than that for other state-of-the-art MOFs, and surpassed the goal set by the US Department of Energy (DOE) (30 g L<sup>−1</sup> by 2020).

Amanda Morris of Virginia Tech, whose research involves MOFs, says, “The report by Chen et al. expands our knowledge of the design principles for hydrogen storage beyond correlations to the surface area. The empirical equations may enable the design of materials that exhibit capacities at the DOE target, thus, providing a pathway to a widely implementable hydrogen economy.” Morris was not involved in this study.

Addressing future directions of this research, Xin Zhang, the first author of the article, says, “Currently, we are targeting new MOFs with optimal pore properties to reach higher hydrogen storage [capacities]. Additionally, we believe that the methodology used to identify the optimal pore volume for hydrogen storage is applicable to the storage-capacity prediction for other gases under various conditions.”

Tianyu Liu

[mrs.org/science-as-art-downloads](https://doi.org/10.1557/mrs.2020.152)

## Bio Focus

**Complex microstructures emerge from chirality and competitive restrictions**

Crystals are generally perceived as objects exhibiting long-range atomic symmetry with overall simple morphologies. As an example, rock salt has a cubic crystallographic structure. Grains of salt encountered in daily life have visibly smooth surfaces. With this perception, morphological complexity in crystals is difficult to imagine and explain. However, sea urchins and marine organisms called coccolithophores display morphological complexity while containing single-crystal components with intricate geometrical shapes. The emergence and existence of such complex geometry in these biological crystals has remained a biomineralization mystery. The surprise stems from the fact that these organisms do not grow from highly defined and size-disperse nanoscale components and, therefore, the wide size distribution is expected to result in disorganized structures. Entropic and enthalpic considerations would further favor random and compact aggregates lacking any morphological distinction.

A team of researchers led by Nicholas A. Kotov at the University of Michigan has now taken a major step toward addressing this question. Kotov says that the study was prompted by the need to better understand the origin of the complexity of inorganic and composite structures in living organisms. “They have to deal with quite ‘messy’ building blocks with wide size distributions, yet demonstrate amazing sophistication in shapes and functions while having very limited means and resources.”

In the study reported in *Science* (doi:10.1126/science.aaz7949), the researchers looked at “chirality” as the potential key enabler of complexity in microparticles. An object is said to be chiral if it is distinct from its mirror image, such as the clockwise-counterclockwise “flavors” of a molecule. To enable complex structures, nanosheets of gold thiolate were synthesized with their surfaces capped with cysteine as ligand molecules. Cysteine is a chiral amino acid that comes in *L*- (clockwise) and *D*- (counterclockwise) flavors. Using either of *L*- or *D*-cysteine, chiral nanosheets were realized that aggregated to give surprisingly complex spiky spheres. On the other hand, using *L*- and *D*-cysteine ligands simultaneously resulted in flat nanosheets

that lacked chirality and led to relatively less complex and flatter morphologies.

“The communities of nanoparticles have to develop complex structures in order to satisfy multiple competitive interactions and restrictions that are imposed on the assembly process. It turns out that in this process, the polydispersity matters less than the symmetry of individual building blocks, which determines the final organization of the building blocks,” Kotov says.

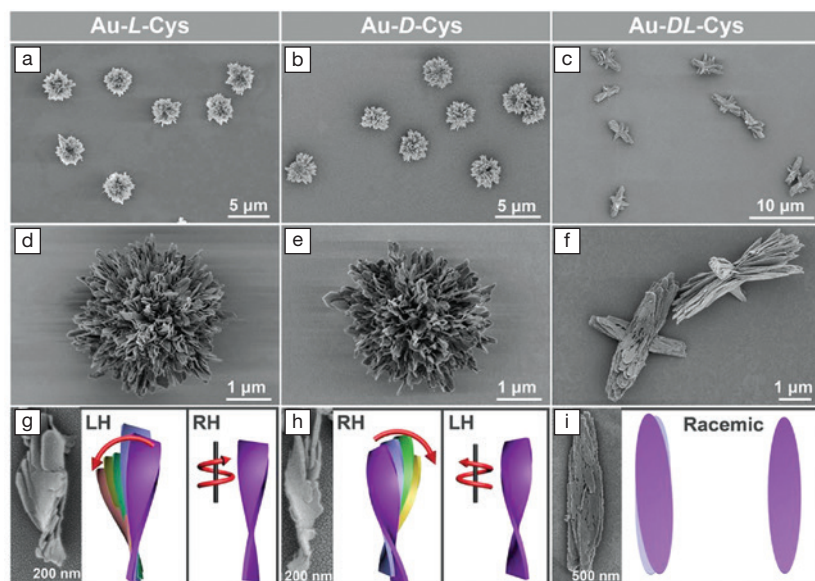
An outstanding aspect of this work is the completeness it provides by explaining the complex structures synthesized and quantifying the emerging complexity. This was enabled by developing computational models that suggested that the spiky spheres made by *L*- or *D*-cysteine are, in fact, among the most complex structures made artificially to date, outcompeting the complexity found in naturally occurring sea urchins and coccolithophores.

“The path to this discovery had to go through enumeration of complexity, which was utterly nontrivial. We developed a method to calculate the complexity of nanoscale assemblies based on graph theory. It allowed us to compare the complexity of different structures that we synthesized and those found in biology rigorously. It turned out that synthetic nano-assemblies can actually outcompete the biological structures in complexity,” Kotov says.

The chirality of these particles provides them with exciting optical and chemical properties. Photons exiting the particles upon light absorption undergo polarization in a two-step process: *first*, due to chirality of the nanosheets, and *second*, due to overall chiral morphology of the microparticle. Furthermore, their spiky geometry and presence of charged ligands result in stable dispersions in both hydrophobic and hydrophilic media, an interesting demonstration of colloidal stability. Kotov says the discovery can have multiple technological consequences.

“It provides the universal energy-efficient path to create numerous complex particles, materials, and, perhaps, even device components. The chiral hedgehog particles that resemble skeletons of marine organisms called coccolithophores can be used in catalysis, optoelectronics, drug delivery, and energy technologies,” Kotov says.

**Ahmad R. Kirmani**



Scanning electron micrographs (SEMs) of microparticles formed by aggregation of (a) *L*-cysteine capped (Au-*L*-Cys), (b) *D*-cysteine capped (Au-*D*-Cys), and (c) *L*,*D*-cysteine capped (Au-*DL*-Cys) gold thiolate nanosheets. (d–f) Enlarged SEMs of (a–c), respectively. (g–i) SEMs of segments of these microparticles with corresponding schematics illustrating their chirality. Credit: *Science*, AAAS, Wenfeng Jiang, The Kotov Lab, University of Michigan.